INTERNATIONAL JOURNAL FOR NUMERICAL METHODS IN FLUIDS, VOL. 17, 839–859 (1993)

A COMPARISON OF NUMERICAL METHODS APPLIED TO NON-LINEAR ADSORPTION COLUMNS

CHRISTOPHE A. POULAIN AND BRUCE A. FINLAYSON

Department of Chemical Engineering, BF-10, University of Washington, Seattle, WA 98195, U.S.A.

SUMMARY

Eight numerical schemes (first-order upstream finite difference, MacCormack, explicit Taylor–Galerkin, random choice, flux-corrected transport, ENO, TVD, and Euler–Lagrange methods) are compared on the basis of their computational efficiency for one-dimensional non-linear convection–diffusion problems. For the ideal chromatographic equation for which an exact solution exists, errors plotted against computational times show that the best methods are the random choice, Euler–Lagrange and flux-corrected MacCormack methods. Even when significant diffusion is added to the model, steep gradients are possible because of non-linearities. In such an instance, the random choice and flux-corrected transport methods give the best performance. One can now tackle more complicated problems and refer to this comparative study in order to choose an adequate numerical method which will provide sufficiently accurate results at a reasonable cost.

KEY WORDS Conservation laws Essentially-non oscillatory methods Total variation diminishing methods Flux-corrected transport methods Random choice method Euler–Lagrange method

INTRODUCTION

Numerical solutions have a distinctive advantage over analytical solutions in that they enable us to solve more complex—and therefore more realistic—problems. For instance, let us consider the case of a chemical species carried along in a plug flow. As a first approximation, one can describe the spatial and temporal changes in concentration of the solute by the linear advection equation which possesses a convenient analytical solution. However, it is possible that axial diffusion will not be negligible, or that the solute will undergo some reaction, as in a tubular reactor. In such event, the relevant model equation might not be solvable analytically, or solutions might exist for a limited number of situations only (e.g. the choice of boundary and/or initial conditions might be restricted). Numerical techniques provide a powerful way to overcome these limitations. Yet, while analytical solutions are exact answers to less complex problems, numerical methods solve more true-to-life problems with some errors. For some situations, these errors can become significant. For example, classical numerical techniques do not work well for linear problems where convection prevails and where the solution moves as a wave limited by steep fronts because, under such conditions, the computed approximations either exhibit large oscillations or are smeared excessively. These difficulties are often exacerbated for non-linear problems. The latter allow the formation of steep gradients and discontinuities even if the initial data is smooth. Furthermore, non-linear problems are difficult to handle because instabilities cannot be predicted by a linearized stability analysis, and the numerical method may predict a solution that is

0271–2091/93/220839–21$15.50

Received 11 November 1992
Revised 14 June 1993

physically unreasonable. Nevertheless, considerable work has been put into devising numerical techniques capable of overcoming the above-mentioned difficulties. The objective of this paper is to compare several numerical methods that a preliminary study[1] has shown to be particularly appropriate for problems marked by strong convection and non-linearity.

The eight schemes studied are: (1) first-order upstream finite difference method; (2) MacCormack method; (3) explicit Taylor–Galerkin method; (4) MacCormack method with flux-correction; (5) Total Variation Diminishing (TVD) method; (6) Essentially Non-Oscillatory (ENO) method; (7) random choice method and (8) Euler–Lagrange method. There are other methods, such as the moving nodes method of Miller and Miller[2,3] and methods using equidistribution principles, such as those by Hu and Schiesser[4] and Smooke and Kozykowski,[5] that have not been applied in this study. Although the qualitative behaviour of the eight schemes we have chosen is well known, it is less clear how their computational efficiencies compare. However, as noted by Fletcher,[6] it is often preferable to estimate the quality of a numerical scheme by considering not only its ability to produce accurate solutions, but also its capacity to produce them quickly.

By applying each of the above methods to a non-linear chromatography problem for which an exact solution is available, we have evaluated their performance with respect to two criteria: accuracy and computational time. The first section of this paper describes the model equation used to test the numerical schemes which are presented in the second section. The last section shows that there is no ideal method. Instead, each method offers a particular trade-off between accuracy and time requirement. If one knows what trade-off is acceptable to solve a given problem, then a computational efficiency diagram, such as the one presented in this study, should provide some help in choosing *a priori* a numerical method suited to the application

MATHEMATICAL MODEL

The difficulties one faces when seeking solutions to models of capillaries in biological tissues provide the motivation for this study. Within each capillary–tissue unit, a set of partial differential equations is solved numerically to predict transport and exchange rates.[7] The problem is complicated by strong axial convection (but there is also diffusion) and non-linear processes governing radial transport and reaction. In addition, proper modelling usually requires solving simultaneously for several units in order to account for the heterogeneity of flow within the organ. But, calculations need to be fast so that investigators can analyse the response of the system to different sets of parameters interactively.[8] Thus, there is a clear need for numerical techniques capable of providing rapid and accurate solutions.

In order to find out which numerical method would best suit these requirements, we have compared several existing schemes by applying them to the closely related problem of non-linear chromatography. Adsorption columns and microvascular vessels are obviously very different physical systems. Nevertheless, the partial differential equations describing the distribution of solute between flowing phase and adsorbant in chromatographic columns[9] are very similar to the equations used in two-region models of capillaries.[10] The general system of equations applicable to both situations is given by equation (1) of Reference 11 when it is written for two compartments (the flowing and stationary phases which are either the solvent and the adsorbent or the blood and the tissues) and where—to account for nonlinearities—the mass transfer and reaction coefficients might depend on the concentrations instead of being constant. For the purpose of this study, we further simplify this model by assuming that: (a) axial diffusion is negligible in the stationary phase, (b) there is no reaction and (c) there is an equilibrium at the interphase. Specifically, the concentration of solute in the fixed phase, c_2, is related to the concentration in the

moving phase, c_1, through the non-linear Langmuir isotherm so that $c_2 = f(c_1) = \alpha c_1/(1+Kc_1)$. With these assumptions, the model reduces to one partial differential equation:

$$\sigma(c_1)\frac{\partial c_1}{\partial \tau} + \frac{\partial c_1}{\partial \xi} = \frac{1}{Pe}\frac{\partial^2 c_1}{\partial \xi^2}, \qquad \tau \geq 0,\ 0 \leq \xi \leq 1, \tag{1}$$

where τ and ξ are dimensionless temporal and spatial variables, respectively, Pe is the Péclet number and $\sigma(c_1)$ is defined as

$$\sigma(c_1) = \frac{\mathrm{d}}{\mathrm{d}c_1}(c_1 + \varepsilon c_2) = 1 + \varepsilon\frac{\mathrm{d}f}{\mathrm{d}c_1} = 1 + \frac{\varepsilon\alpha}{(1+Kc_1)^2}, \tag{2}$$

where $\varepsilon = V_2/V_1$ denotes the ratio of the volume of the stationary phase to that of the flowing phase. Equation (1) is solved for its single unknown, c_1. Once the concentration of solute in the moving fluid is known, the concentration in the fixed phase directly follows from the equilibrium relation. The auxiliary conditions associated with Equation (1) are:

$$c_1(\xi, 0) = \mathrm{i}(\xi),\ c_1(0, \tau) = b(\tau) \text{ and } \left(\frac{\partial c_1}{\partial \xi}\right)_{\xi=1} = 0. \tag{3}$$

Note that, in chromatography, a boundary condition more frequently used at the inlet is the Danckwerts boundary condition:[12]

$$c_1(0, \tau) - \frac{1}{Pe}\left(\frac{\partial c_1}{\partial \xi}\right)_{\xi=0} = b(\tau), \tag{4}$$

but with convection dominating over diffusion (i.e. for large Pe number) this is essentially $c_1(0, \tau) = b(\tau)$, which is the condition we used.

An even simpler model is derived when axial diffusion in the flowing phase is assumed to be negligible.[13,14] Then the right-hand side of equation (1) is replaced by zero and the boundary condition at the outlet is dropped. The resulting problem is often referred to as the ideal, non-linear chromatography model.[15] Although its physical significance is somewhat limited, this model provides an interesting test for the numerical methods we intend to compare. Since, for certain choice of auxiliary conditions, there exist exact solutions to equation (1) where the diffusion term has been removed, it is possible to analyse quantitatively the performance of the numerical methods. The ideal, non-linear chromatogrphic equation also constitutes a good test because it has the ability to produce solutions with discontinuities or shocks. Since these are always a source of numerical difficulties, it will be instructive to see how well the numerical schemes can handle them. Moreover, if the methods perform well in the limiting case where there is no axial diffusion, they should also produce good results for actual situations where shocks do not occur but very steep gradients are observed. Ma and Guiochon[16] mention that for typical columns in High-Pressure Liquid Chromatography (HPLC) apparent axial dispersion coefficients are in the range from 1 to $6 \times 10^{-4}\ \mathrm{cm^2\,s^{-1}}$, which combined with a fluid velocity of $0{\cdot}15\ \mathrm{cm\,s^{-1}}$ and a column length of 15 cm (these are the values used in their simulation), places the Péclet number between 22 500 and 3750. Sometimes, however, the Péclet number is not that large. In capillaries of the heart, for example, typical values of the effective Péclet number for axial diffusion are in the range from 100 to 1000. Thus, numerical schemes are needed that not only perform well in the ideal case, but can also account for a large range of axial diffusion.

THEORETICAL RESULTS

Test problem: exact concentration profiles

The most obvious way to study the accuracy of a numerical method is to compare the computed approximation to an exact answer. Thanks to the method of characteristics, it is possible to construct (at least for times not too large) the exact solution to the ideal chromatographic equation when some solute is injected into a clean column. The corresponding auxiliary conditions are:

$$c_1(\xi, 0)=0 \text{ and } c_1(0, \tau)=\begin{cases} c_{in} & \text{if } 0\leq\tau\leq\tau_i, \\ 0 & \text{if } \tau>\tau_i. \end{cases} \tag{5}$$

The situation is depicted in Figure 1. At the initial time, a discontinuity appears at $\xi=0$. Since the equilibrium isotherm we have chosen is convex upward, Rhee *et al.*[9] show that the so-called entropy condition (that is the condition under which a discontinuity is a shock) is $\sigma(c_1^{\ell})\leq\sigma(c_1^{r})$, where the superscripts ℓ and r denote, respectively, the left and right side of the discontinuity. For the Langmuir isotherm, this condition simplifies to: $c_1^{\ell}\geq c_1^{r}$. Thus, from the discontinuity at ($\xi=0$, $\tau=0$), a genuine shock forms that will propagate with speed v_s given by the jump condition:

$$v_s=\frac{[c_1]}{[g(c_1)]}=\frac{c_1^{\ell}-c_1^{r}}{g(c_1^{\ell})-g(c_1^{r})}. \tag{6}$$

Here, the function $g(c_1)$ stands for the sum $c_1+\varepsilon f(c_1)$. g is sometimes called the column *isotherm*. Equation (6) also introduces the notation $[\cdot]$ which is traditionally used to indicate the jump across the discontinuity of a given quantity.

At the moment when the solute injection is stopped, another discontinuity appears at the inlet of the column. Since this time the entropy condition is not satisfied, the discontinuity gives rise to a centred simple wave that will expand. In the (ξ, τ)-plane that wave is represented by a manifold of straight characteristics emanating from the same point $(0, \tau_i)$ and having slope $(d\tau/d\xi)=\sigma(c_1)$, where c_1 varies from 0 to c_{in}. For a given value of the solute concentration, however, the slope $d\tau/d\xi$ is constant and is equal to $(\tau-\tau_i)/\xi$. Therefore, for any point in the centred wave, the solute concentration is given by

$$c_1=-\frac{1}{K}\left[1-\sqrt{\left(\frac{\varepsilon\alpha}{(\tau-\tau_i)/\xi-1}\right)}\right]. \tag{7}$$

We note that the largest speed in the rarefaction wave, $1/\sigma(c_{in})$, is greater than the shock velocity. This means that the trailing wave moves faster than the discontinuity and, ultimately, will catch up with it. Prior to the catch-up time T, the jump in concentration across the shock is constant. Thus, the shock path in the plane of the characteristics is a straight line. At time T, the characteristic from the centred wave bearing the concentration c_{in} intersects the shock path. This corresponds to the situation depicted in Figure 1(c): the expansion wave has just caught up with the front. For the later time ($\tau>T$), the intensity of the shock decreases, as Figure 1(d) shows, and the shock path is not straight anymore.

For the quantitative part of our analysis, we will limit ourselves to times below T. Therefore, the concentration profiles we will compute should resemble the one displayed in Figure 1(b). The solution includes three constant states separated by an expansive wave and a shock discontinuity.

Solute quantities and their variations

Most of the numerical methods compared in this study have been designed to solve hyperbolic conservation laws of the form $u_\tau+F(u)_\xi=0$. If we define $\langle u\rangle$ as the total amount of the quantity

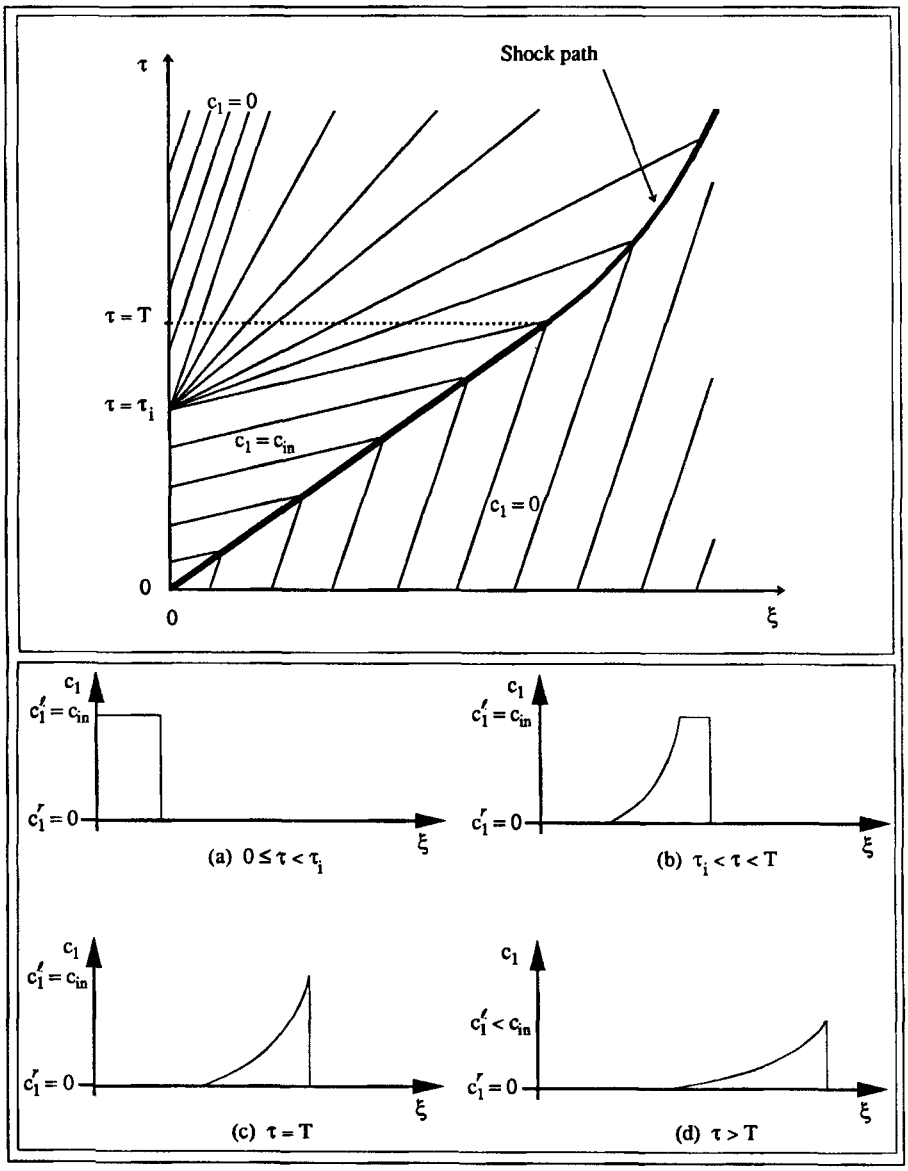

Figure 1. Characteristics (upper panel) and concentration profiles at various instants (lower panels) for the injection of a fixed quantity of solute into an ideal column initially clean, equation (5). c_1^l and c_1^r are the values of the concentration to the left and right of the discontinuity, respectively; T is the time until which the intensity of the shock remains constant.

u in some closed region, then the fundamental assumption underlying the conservation law is that the rate of change of $\langle u \rangle$ is equal to the net flux of u across the boundaries of that region.[17] This must hold whether u is smooth or not. It is an important fact to consider if we want to apply correctly the conservative numerical schemes to the non-linear chromatographic equation in the presence of discontinuous concentration curves.

In the absence of diffusion, it is easy to write equation (1) in divergence form as

$$\frac{\partial R(c_1)}{\partial \tau}+\frac{\partial S(c_1)}{\partial \xi}=0. \tag{8}$$

One can pick any pair of functions (R, S) provided $R'(c_1)$ equals $[1+\varepsilon f'(c_1)]S'(c_1)$. Three possibilities easily come to mind. R could be set to be (1) the concentration of solute in the moving phase, c_1; (2) the concentration of solute in the stationary phase, $c_2=f(c_1)$; or (3) the combination of these two concentrations defined earlier, $g(c_1)$. For the sake of clarity, we will say that equation (1) with no diffusion is written in the $\mathscr{C}1$-form, $\mathscr{C}2$-form or $\mathscr{G}$-form if $R(c_1)$ is c_1, c_2 or $g(c_1)$, respectively. This notation is summarized in Table I.

We might regard these three forms of the ideal chromatographic equation as perfectly equivalent conservation laws since they all represent the same physical phenomena. The $\mathscr{C}1$-form is particularly attractive since its solution provides directly the solute concentration in the flowing phase which is the quantity we are seeking. However, only the $\mathscr{G}$-form of the conservation law is physically acceptable. Let us consider a chromatographic column for which a fraction ϕ of the total volume is occupied by the flowing phase. Then the quantity $G=\phi g$ represents the total concentration of solute (held both in solution and in adsorbant) at a given time and point in the column. In addition, a mass balance carried over the entire system shows that $\langle G\rangle$, the total mass of solute in the chromatographic column, varies only when solute is fed into the column or exists from it. On the other hand, since mass is constantly transferred between moving and stationary phases as bands of solute propagate along the column, there is, in the general case, no physical reason indicating that the time variations of the quantities $\langle c_1\rangle$ and $\langle c_2\rangle$ should be equal to the net flux of solute entering the system. Therefore, while the three forms of equation (8) are all mathematically correct conservation laws, physical insights indicate that the $\mathscr{G}$-form of the model equation is the right form to use in order to obtain meaningful results.[18]

Table I. Three possible ways to put the ideal, non-linear chromatographic equation into the form of equation (8) and the corresponding first-order upstream finite difference schemes

Form	$R(c_1)$	$S(c_1)$	Finite difference algorithm. knowing c_1^n, find c_1^{n+1} with:
$\mathscr{C}1$	c_1	$M(c_1)=\int_0^{c_1}\frac{du}{1+\varepsilon f'(u)}$	$c1_i^{n+1}=c1_i^n-\frac{\Delta\tau}{\Delta\xi}[M(c1_i^n)-M(c1_{i-1}^n)]$
$\mathscr{C}2$	$c_2=f(c_1)$	$N(c_1)=\int_0^{c_1}\frac{f'(u)\,du}{1+\varepsilon f'(u)}$	(1) $c2_i^n=\frac{\alpha c1_i^n}{1+Kc1_i^n}$; (2) $c2_i^{n+1}=c2_i^n-\frac{\Delta\tau}{\Delta\xi}[N(c1_i^n)-N(c1_{i-1}^n)]$; (3) $c1_i^{n+1}=\frac{c2_i^{n+1}}{\alpha-Kc2_i^{n+1}}$
$\mathscr{G}$	$g(c_1)=c_1+\varepsilon f(c_1)$	$\int_0^{c_1}du=c_1$	(1) $g_i^n=c1_i^n\left(1+\frac{\varepsilon\alpha}{1+Kc1_i^n}\right)$; (2) $g_i^{n+1}=g_i^n-\frac{\Delta\tau}{\Delta\xi}[c1_i^n-c1_{i-1}^n]$; (3) $c1_i^{n+1}=\begin{cases}\frac{g_i^{n+1}}{1+\varepsilon\alpha}\text{ if } K=0\\ \frac{1}{2K}[Kg_i^{n+1}-1-\varepsilon\alpha+\sqrt{[(Kg_i^{n+1}-1-\varepsilon\alpha)^2+4Kg_i^{n+1}]}]\\ \text{if } K>0\end{cases}$

Let us conclude by emphasizing that in our definition of the $\mathscr{G}$-form the variable is the column isotherm, g, and the flux is a function of that variable $c_1 = g^{-1}(g)$. This is different from the approach of Rouchon *et al.*[15] who, by reversing the role of τ and ξ, considered an equation in the $\mathscr{G}$-form but with c_1 as the variable and $g(c_1)$ as the flux function. Our approach has the inconvenient feature that, in the solution process, we must at each time step go from c_1 to g and back from g to c_1. Although this does not increase the computational load very much (see section on MacCormack method below), it can become problematic if there is no easy way to obtain c_1 from g. However, it has the marked advantage that axial diffusion can be included.

NUMERICAL METHODS

We now describe the numerical methods as applied to the model of single solute chromatography with non-linear equilibrium (equations (1)–(3) with or without diffusion). In the first part, we present numerical methods for conservation laws which require the model equation to be put into the $\mathscr{G}$-form defined earlier. In particular, because of its simplicity, the first-order upstream finite difference scheme is used to illustrate the general features associated with the application of conservative methods to the chromatographic equation. In a second part, we report on two schemes (random choice method and explicit Euler–Lagrange method) which can be applied to the more general class of hyperbolic equations. With the exception of the Euler–Lagrange method, all the schemes are implemented on a fixed mesh.

Conservative numerical methods

For fixed grid methods, the domain where the solution is sought is replaced by a regular mesh $\{(\xi_i = i\Delta\xi,\ \tau^n = n\Delta\tau) \mid i = 0, 1, \ldots, N_s \text{ and } n = 0, 1, \ldots,\}$. The grid spacing is simply $\Delta\xi = 1/N_s$, since ξ belongs to $[0; 1]$. The purpose of the numerical method is to provide, at each node, an approximation $u_i^n = u(\xi_i, \tau^n)$ to the exact solution $u_{ex}(\xi_i, \tau^n)$.

First-order upstream finite difference method. This finite difference method has the advantage of being straightforward and easy to implement. To evaluate the first derivative of the convection term, upstream weighting is preferred to central differencing because that provides some stability by introducing a certain amount of artificial diffusion. The latter helps dampen any oscillation. However, if too much numerical viscosity is added, then the solution is smoothed excessively. With the explicit Euler method to step forward in time, the scheme written for the general conservation law, $u_\tau + F(u)_\xi = 0$, is

$$u_i^{n+1} = u_i^n - \frac{\Delta\tau}{\Delta\xi}(\mathscr{F}_i^n - \mathscr{F}_{i-1}^n), \tag{9}$$

where the consistent flux function is simply $\mathscr{F}(u_i^n) = F(u_i^n)$. Equation (9) defines the typical structure of a conservative finite difference method.[18] Writing this equation over all values of i and summing gives

$$\langle u \rangle^{n+1} = \langle u \rangle^n - \Delta\tau(\mathscr{F}_{N_s}^n - \mathscr{F}_1^n), \tag{10}$$

where $\langle u \rangle = \sum u_i$. This is the discrete equivalent of the fundamental assumption underlying every conservation law, and meaning that the temporal variations of the total amount of the quantity u in the system are solely dependent on the net flux of material at the inlet and outlet of that system. Consequently, conservative methods must be applied to the $\mathscr{G}$-form of the chromatographic equation.

To illustrate the disastrous (and insidious) effects of choosing the physically wrong form of the conservation law, we have used the first-order upstream finite difference scheme to solve the ideal chromatographic equation put into each of the three forms defined in the previous section. The complete algorithms are summarized in Table I. Typical solutions for the elution of a partially saturated column are displayed in Figure 2(a). Although the three concentration profiles have the same shape, the position of the front is different. Figure 2(b) shows that this is not due to a lack of accuracy, since, in the limit where $\Delta\tau$ and $\Delta\xi$ go to zero, the front velocity computed with each form of the finite difference scheme converges to the shock speed predicted by the Rankine–Hugoniot relationship written for the corresponding hyperbolic conservation law. In

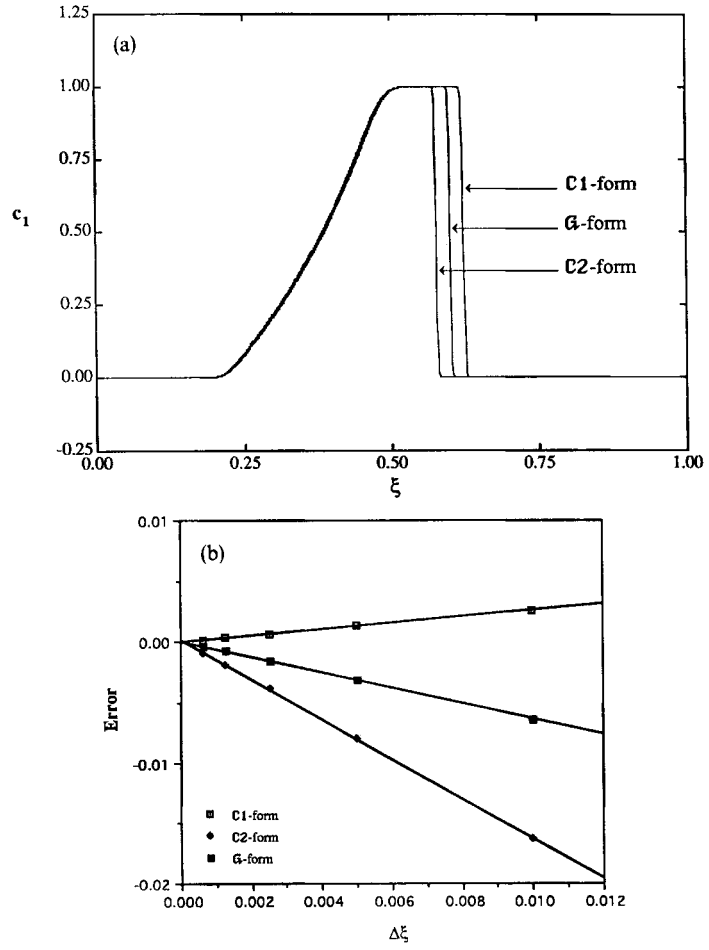

Figure 2. (a) Comparison of the numerical solutions provided by the three finite difference algorithms of Table I for the elution of a chromatographic column saturated ($c_1 = 1$) between $\xi = 0{\cdot}10$ and $\xi = 0{\cdot}35$ and clean ($c_1 = 0$) everywhere else. $\alpha = 2$, $K = 2$, $\varepsilon = 1{\cdot}5$, $\Delta\xi = 1/800$, $\Delta\tau/\Delta\xi = 1$. Solutions are shown at time $\tau_{obs} = 0{\cdot}5$. (b) Error in the propagation speed of the front for different grid spacing. The conditions are the same as in Figure 2(a) except for $\Delta\xi$ which varies from 1/100 to 1/1600. The error is defined as $(v - v_X)$, where v is the computed mean velocity between $\tau = 0$ and $\tau = 0{\cdot}4$ and v_X is the analytical value of the Rankine–Hugoniot shock speed for the conservation law written in the X-form with $X = \mathscr{C}1$, $\mathscr{C}2$ or $\mathscr{G}$. In the numerical approximation the front is located where $c_1 = (c_1^f + c_1^r)/2$ and $(\partial c_1/\partial\xi) < 0$.

fact, with Lax and Wendroff's theorem,[19] one can show that the approximations provided by the numerical method in the $\mathscr{C}1$-, $\mathscr{C}2$- and $\mathscr{G}$-form converge to the entropy satisfying weak solution of the conservation law written in the same form (since the flux functions M, $N \circ f^{-1}$ and g^{-1} are all convex, the entropy condition is merely $u^{\ell} > u^{r}$ for $u = c_1$, c_2 and g). As a result, only the solution provided by the $\mathscr{G}$-form is physically acceptable.

We finish the description of the finite difference method by indicating how it can be extended to include diffusion. It is easily done by noting that the modelling equation with a diffusion term is also a conservation law (however, it is no longer hyperbolic):[18]

$$\frac{\partial g}{\partial \tau} + \frac{\partial c_1}{\partial \xi} - \frac{1}{Pe}\frac{\partial^2 c_1}{\partial \xi^2} = \frac{\partial g}{\partial \tau} + \frac{\partial}{\partial \xi}\left(c_1 - \frac{1}{Pe}\frac{\partial c_1}{\partial \xi}\right) = 0. \tag{11}$$

Thus, we need only modify the numerical flux function as

$$\mathscr{F}_i^n = c1_i^n - \frac{c1_{i+1}^n - c1_i^n}{Pe\Delta\xi} \tag{12}$$

MacCormack method. The MacCormack method is a difference scheme using two steps to achieve second-order accuracy in both space and time. It was introduced to solve the time-dependent compressible Navier–Stokes equations.[20] Its application to the adsorption problem has been derived by Finlayson.[1] For the $\mathscr{G}$-form of equation (1), the method reads:

$$g_i^{*n+1} = g_i^n - \frac{\Delta\tau}{\Delta\xi}(c1_{i+1}^n - c1_i^n) + \frac{\Delta\tau}{Pe\Delta\xi^2}(c1_{i+1}^n - 2c1_i^n + c1_{i-1}^n)$$

$$g_i^{n+1} = \frac{1}{2}\left[(g_i^n + g_i^{*n+1}) - \frac{\Delta\tau}{\Delta\xi}(c1_i^{*n+1} - c1_{i-1}^{*n+1}) + \frac{\Delta\tau}{Pe\Delta\xi^2}(c1_{i+1}^{*n+1} - 2c1_i^{*n+1} + c1_{i-1}^{*n+1})\right]. \tag{13}$$

The addition of diffusion follows work by Anderson *et al.*[21] on viscous Burgers equations. Note that the two equations above can easily be recast into one equation similar to equation (9) showing the conservative property of the MacCormack method. Like all the conservative schemes of this section, the MacCormack method enable us to evaluate g^{n+1} from g^n. However, the complete solution process involves two additional steps: (1) obtain g^n from c_1^n; and (2) deduce c_1^{n+1} from g^{n+1}. Although necessary, these two steps do not increase the computational load very much since: (1) except at the starting time, when g^0 is not known, g^n and c_1^n are already known from the previous time level; and (2) by going from g^{n+1} to c_1^{n+1}, we actually compute the numerical flux for the next time level and this is a calculation that would have to be done anyway with a conservative scheme except, of course, when the final time has been reached.

Taylor–Galerkin method. Galerkin finite element solutions to convection-dominated problems often exhibit undesirable oscillations. Noting that this might be caused by the finite difference approximation of the time derivative, Donea[22,23] created a way to improve typical time-stepping methods. This was achieved by using Taylor series expansions to evaluate the time derivative. The derivation of the method for the adsorption problem requires special formulae in order to expand the nonlinear terms in terms of the trial functions N_i. Finlayson[1,24] found that the following scheme worked well:

$$\left(\frac{dc_1}{dg}\right)^2_{(\xi,\tau)} = \sum_k \left(\frac{dc_1}{dg}\right)^2_{(k\Delta\xi,\tau)} N_k(\xi). \tag{14}$$

Finally, the complete scheme is

$$\tfrac{1}{6}(g_{i+1}^{n+1}-g_{i+1}^{n})+\tfrac{2}{3}(g_i^{n+1}-g_i^{n})+\tfrac{1}{6}(g_{i-1}^{n+1}-g_{i-1}^{n})=-\frac{\Delta\tau}{\Delta\xi}(\mathscr{F}_i^n-\mathscr{F}_{i-1}^n)$$

$$\mathscr{F}_i^n=\tfrac{1}{2}[c1_{i+1}^n+c1_i^n]-\frac{\Delta\tau}{4\Delta\xi}\left[\left(\left(\frac{dc_1}{dg}\right)_{i+1}^n\right)^2+\left(\left(\frac{dc_1}{dg}\right)_i^n\right)^2\right][g_{i+1}^n-g_i^n]-\frac{c1_{i+1}^n-c1_i^n}{Pe\Delta\xi}. \quad (15)$$

When the left-hand side of the equation (15) is 'lumped', the Taylor–Galerkin method is clearly a conservative and consistent finite difference method. To show that the finite element version without lumping also underlies a conservation principle, let us assume that the solution u to the general conservation law $u_\tau+F(u)_\xi=0$ is constant everywhere outside some finite interval $[\xi_j, \xi_k]$. The total quantity of u within the interval $[\xi_{j-m}; \xi_{k+m}]$ is

$$\langle u\rangle_{(j-m;\,k+m)}=\int_{\xi_{j-m}}^{\xi_{k+m}} u\,d\xi\approx\sum_{i=j-m+1}^{k+m}u_i\Delta\xi. \quad (16)$$

Summing equation (15) (written in the general case, i.e. by replacing g and c_1 by u and $F(u)$ respectively) for i ranging from $j-m+1$ to $k+m$, we obtain

$$\tfrac{1}{6}\Delta u_{j-m}+\tfrac{5}{6}\Delta u_{j-m+1}+\sum_{i=j-m+2}^{k+m-1}\Delta u_i+\tfrac{5}{6}\Delta u_{k+m}+\tfrac{1}{6}\Delta u_{k+m+1}=-\frac{\Delta\tau}{\Delta\xi}(\mathscr{F}_{k+m}-\mathscr{F}_{j-m}). \quad (17)$$

where $\Delta u=u^{n+1}-u^n$. Since u is constant outside $[\xi_j, \xi_k]$, we have, for m large enough: $\Delta u_{j-m}=\Delta u_{j-m+1}$ and $\Delta u_{k+m}=\Delta u_{k+m+1}$. Therefore, equation (17) reduces to

$$-\Delta\tau(\mathscr{F}_{k+m}-\mathscr{F}_{j-m})=\Delta\xi\sum_{i=j-m+1}^{k+m}\Delta u_i=\langle u\rangle_{(j-m;\,k+m)}^{n+1}-\langle u\rangle_{(j-m;\,k+m)}^{n} \quad (18)$$

showing that the variations of the total quantity of u within the region considered depend on the net flux of u across the boundaries of that domain.

Flux-corrected transport. With the flux-corrected transport method, we switch to a class of conservative schemes referred to as high-order or high-resolution methods. To belong to that category, a numerical method must be at least second-order accurate away from the front and be able to keep the front steep without any oscillation.[18]

To achieve a high-resolution, the flux-corrected transport method tries to average two kinds of numerical fluxes: (1) high-order fluxes from schemes that can keep the front steep but oscillate and (2) low-order fluxes from methods that do not oscillate but smooth the front excessively.[1,25] A flux-correction step can be added to any method. To a certain extent, it acts like a filter that would eliminate unwanted oscillations or overcome excessive smearing.

The version we use in this study follows work by Book and Boris.[26,27] The flux-correction is applied to the MacCormack method, equation (13), according to equations (6.22)–(6.29) of Reference 1 when the variable u is replaced by the column isotherm, g, and the numerical flux function, $u_i^2/2$, is changed to $c1_i$ for the ideal model or $c1_i-(c1_{i+1}-c1_i)/(Pe\Delta\xi)$ in the presence of diffusion.

Total variation diminishing methods. The fact that a numerical method is Total Variation Diminishing (TVD) is sufficient to ensure that the method is stable (precisely TV-stable). If in addition, it is consistent and conservative then convergence is guaranteed.[18] These properties have served as foundations for a great variety of TVD schemes. The key in the development of these methods lies in the choice of the numerical flux. The latter must be limited so that the total

variation of the method does not increase. The basis for this type of high-order methods have been explained by Harten, Yee *et al.* and Sweby.[28-30]

The TVD method used in this study is a second-order method explained in Chen *et al.*[31] A second-order Runge–Kutta method is employed to move the solution forward in time. The algorithm applied to the general conservation law, $u_\tau + F(u)_\xi = 0$, is described by Finlayson[1] (equations (6.92)–(6.101)). The application of the TVD scheme to the chromatographic equation requires to (1) compute $g^n = g(c_1^n)$; (2) advance the solution by one time level with the TVD scheme where the general variables u and $F(u)$ have been replaced by the appropriate unknown and numerical flux, as shown for the FCT scheme and (3) go back from g to c_1 with $c_1^{n+1} = g^{-1}(g^{n+1})$.

Essentially non-oscillatory method. ENO methods also belong to the class of high-resolution methods. Shu and Osher have presented several versions of ENO methods.[32,33] The simplest of them, namely the third-order ENO–Roe method, is used here. Integration in time proceeds with a third-order Runge–Kutta method. In space, however, the scheme consists in finding a third-order polynomial, $P_3(\xi)$, which interpolates the set of values $H(\xi_{i+1/2})$. Here, H is the primitive function of $h(\xi)$ which is such that

$$F(u(\xi)) = \frac{1}{\Delta\xi} \int_{\xi-\Delta\xi/2}^{\xi+\Delta\xi/2} h(y)\,\mathrm{d}y. \tag{19}$$

Then, the net flux going into the cell between $\xi_{i-1/2}$ and $\xi_{i+1/2}$ is simply $\mathscr{F}_{i+1/2} - \mathscr{F}_{i-1/2} = P_3'(\xi_{i+1/2}) - P_3'(\xi_{i-1/2})$. To avoid the formation of oscillations, P_3 is constructed in an ENO fashion. The complete scheme for a conservation law of the form, $u_\tau + F(u)_\xi = 0$, is given by equations (6.107)–(6.124) of Reference 1. These can be easily modified to solve the $\mathscr{G}$-form of the chromatography problem, as described earlier.

It is important to note that the ENO methods of Shu and Osher were designed with periodic boundary conditions. Although these are necessary to determine P_3, they are not suitable for the modelling of adsorption columns. To overcome that difficulty, Finlayson[1] proposes to use lower-order formulae at the inlet and outlet of the domain. Thus, for the second ($j=1$) and next to last ($j=N_s-1$) points, we replace the third-order polynomial P_3 by a polynomial of degree 2 and, for the last node ($j=N_s$), we use a polynomial of degree one.

Other numerical methods

Unlike conservative methods which must be used with the physically right form of a conservation law, the two schemes presented below can be applied to any form of equation (1). The $\mathscr{C}1$-form, however, is the most appropriate since its solution directly provides the moving phase concentration, c_1, which is the quantity measured experimentally.

Random choice method. As reported by Holt,[34] many authors have contributed to the development of the random choice method.[34-40] The version presented below proceeds in two steps. At each time level n and for each grid point ξ_i, a Riemann problem defined by the ideal model in the $\mathscr{C}1$-form and the initial condition:

$$c_1 = \begin{cases} c1_i^n & \text{if } \xi < \xi_i + \Delta\xi/2 \\ c1_i^{n+1} & \text{if } \xi \geq \xi_i + \Delta\xi/2 \end{cases} \tag{20}$$

is first solved. The solution at $(\xi_{i+1/2} + \theta_{2n+1}\Delta\xi,\ \tau^n + \Delta\tau/2)$ is called

$$c1_{i+1/2}^{n+1/2} = w(\xi_{i+1/2} + \theta_{2(n+1/2)}\Delta\xi,\ \tau^{n+1/2}). \tag{21}$$

The procedure is then repeated. Another set of Riemann problems is formed and, from the values

of the intermediate solution at nodes $(i-1/2)$ and $(i+1/2)$, we deduce the new value of the concentration: $c1_i^{n+1} = w(\xi_{i+1} + \theta_{2(n+1)}\Delta\xi, \tau^{n+1/2})$.

In the expressions above, θ is a random variable. Its purpose is to note that, on a fixed grid, a discontinuity arising from a shock might be located between two nodes. Thus, after one full time step, the solution can be off a distance $\Delta\xi/2$ and such errors can accumulate. But this can be avoided by placing the front at random points uniformly distributed around the true location of the discontinuity. Holt remarks that the accuracy of the random choice method improves when the θ's are close to equidistribution on $[-1/2; 1/2]$.[34] Colella found that the best procedure to select θ is provided by the van der Corput sequence.[41] This was confirmed by Finlayson.[1]

When applied to hyperbolic equations, the random choice method has the advantge of being unconditionally stable. Nevertheless, in order to construct a global solution by superposing the solutions of the individual Riemann problems, it is necessary that the Courant–Friedrichs–Lewy (CFL) condition be satisfied. For the $\mathscr{C}1$-form of the ideal chromatographic equation, this is

$$\frac{v_{\max}\Delta\tau}{\Delta\xi} \leq 1, \quad v_{\max} = \operatorname*{Max}_i \left\{ \frac{1}{\sigma(c1_i)} \right\}. \tag{22}$$

The random choice method also has the advantage that it does not introduce numerical diffusion. Therefore, a discontinuity can be convected without deformation.

It remains that the performances of the random choice method strongly depend on our ability to solve the Riemann problem accurately and rapidly. For the chromatography problem, there is a convenient approximate solution:

$$\text{If } c1_\ell^{k-1/2} \geq c1_r^{k-1/2},\ w(\xi+\theta\Delta\xi, \tau^k) = \begin{cases} c1_\ell^{k-1/2} & \text{for } \theta\Delta\xi < \tfrac{1}{2} v_s \Delta\tau, \\ c1_r^{k-1/2} & \text{for } \theta\Delta\xi \geq \tfrac{1}{2} v_s \Delta\tau, \end{cases}$$

$$\text{If } c1_\ell^{k-1/2} < c1_r^{k-1/2},\ w(\xi+\theta\Delta\xi, \tau^k) = \begin{cases} c1_\ell^{k-1/2} & \text{for } \theta\Delta\xi < \tfrac{1}{2} v_\ell \Delta\tau, \\ c1_r^{k-1/2} & \text{for } \theta\Delta\xi \geq \tfrac{1}{2} v_r \Delta\tau, \\ \tfrac{1}{2}(c1_\ell^{k-1/2} + c1_r^{k-1/2}) & \text{otherwise.} \end{cases} \tag{23}$$

The derivation of this equation follows work by Sod on non-linear Burgers equation.[15] $c1_\ell$ and $c1_r$ denote the left and right states of the Riemann problem. v_s is the shock speed. v_ℓ and v_r are the velocities to the left and to the right of the Riemann solution, respectively. Note that, in opposition to methods in conservation form, the random choice method requires these three velocities to be known explicitly. For the adsorption problem they are

$$v_s = \left[1 + \varepsilon \frac{f(c1_\ell^{k-1/2}) - f(c1_r^{k-1/2})}{c1_\ell^{k-1/2} - c1_r^{k-1/2}} \right]^{-1}, \quad v_\ell = \frac{1}{\sigma(c1_\ell^{k-1/2})} \quad \text{and} \quad v_r = \frac{1}{\sigma(c1_r^{k-1/2})}. \tag{24}$$

The fact that v_s, v_ℓ and v_r are strictly positive can be used to lower the computational time. Indeed, when the van der Corput sequence is used in the way recommended by Holt,[31] the value of θ turns out to be positive when the solution is advanced from τ^n to $\tau^{n+1/2}$ and strictly negative when it is advanced from $\tau^{n+1/2}$ to τ^{n+1}. Thus, in the second case ($\theta < 0$), the solution to the Riemann problem at each node is simply the left state and no calculation needs to be preformed.

It should also be noted that for the ideal chromatographic equation there is an exact solution to the Riemann problem. Equation (23) represents a more general formulation since, in many other applications, the Riemann problem cannot be solved exactly. Furthermore, we found that results obtained with both the exact and the approximate Riemann solutions were almost identical. Therefore, we only show results obtained with Sod's approximate solution.

When there is diffusion, the hyperbolic equation is first solved according to the preceding explanations and the solution is called $c1^*$. Then a diffusion step is added to give the final solution[1]

$$\frac{c1_i^{n+1}-c1_i^{*n+1}}{\Delta\tau}=\frac{c1_{i+1}^{*n+1}-2c1_i^{*n+1}+c1_{i-1}^{*n+1}}{\sigma(c1_i^{*n+1})Pe\Delta\xi^2}. \tag{25}$$

Explicit Euler–Lagrange method. The Euler–Lagrange method uses a moving mesh. To start, we rewrite the modelling equation as

$$\frac{Dc_1}{D\tau}=\frac{\partial c_1}{\partial\tau}+\frac{1}{\sigma(c_1)}\frac{\partial c_1}{\partial\xi}=\frac{1}{\sigma(c_1)}\frac{1}{Pe}\frac{\partial^2 c_1}{\partial\xi^2}. \tag{26}$$

Then, following work by Thomaidis *et al.*,[42] an explicit scheme is used to solve the diffusion step:

$$\left(\frac{Dc1_i}{D\tau}\right)^n=\frac{{}_ic1^{n+1}-c1_i^n}{\Delta\tau}=\frac{1}{\sigma(c1_i^n)}\frac{1}{Pe}\frac{\dfrac{c1_{i+1}^n-c1_i^n}{\Delta\xi_i^n}-\dfrac{c1_i^n-c1_{i-1}^n}{\Delta\xi_{i-1}^n}}{\frac{1}{2}(\Delta\xi_i^n+\Delta\xi_{i-1}^n)}. \tag{27}$$

Note that the grid spacing $\Delta\xi$ has been replaced by $\Delta\xi_i=\xi_{i+1}-\xi_i$, since in a moving grid the distance between two nodes can vary. In the expression above, we have also introduced a special notation, namely ${}_ic1^{n+1}$. This is because equation (27) provides values of the concentration at the new time but on the old mesh. In order to obtain the final solution we need to add the convection step:

$$\xi_i^{n+1}=\xi_i^n+v_i^n\Delta\tau. \tag{28}$$

This is equivalent to moving the solution along the appropriate charateristic. Thus, the velocity v in the relation above will, in general, be $1/\sigma(c1_i^n)$. When there is a shock, however, the shock speed must be calculated according to equation (6).

Therefore, one of the difficulty with this version of the Euler–Lagrange method is that we must be able to know, at each time step, if there is a shock and, if so where it is. In addition, since nodes move with different speeds, two successive points can either become too distant or too close (and eventually cross). Thus, we need to be able to add nodes to keep a good resolution and to remove nodes so that the grid spacing is kept to a minimum value. All these constraints tend to make the programming of the method quite arduous.

RESULTS AND DISCUSSION

Ideal model

All the numerical methods described above have been used to solve the test problem outlined in Section 1. Typical results are displayed in Figure 3(a)–(3h). The MacCormack method and the explicit Taylor–Galerkin method lead to solutions which oscillate. Typically, the 'lumped' Taylor–Galerkin scheme gives the largest overshoot. When no lumping is used, the overshoot is less important but the wiggles are more spread out. The other six methods do not exhibit oscillations. Instead, the first-order upstream finite difference and the TVD methods introduce a significant amount of numerical diffusion. The ENO and FCT solutions are also smoothed. However, the front discontinuity is kept steep and the sharp angles at each end of the rarefaction wave are not rounded excessively. The random choice and Euler–Lagrange methods give the best

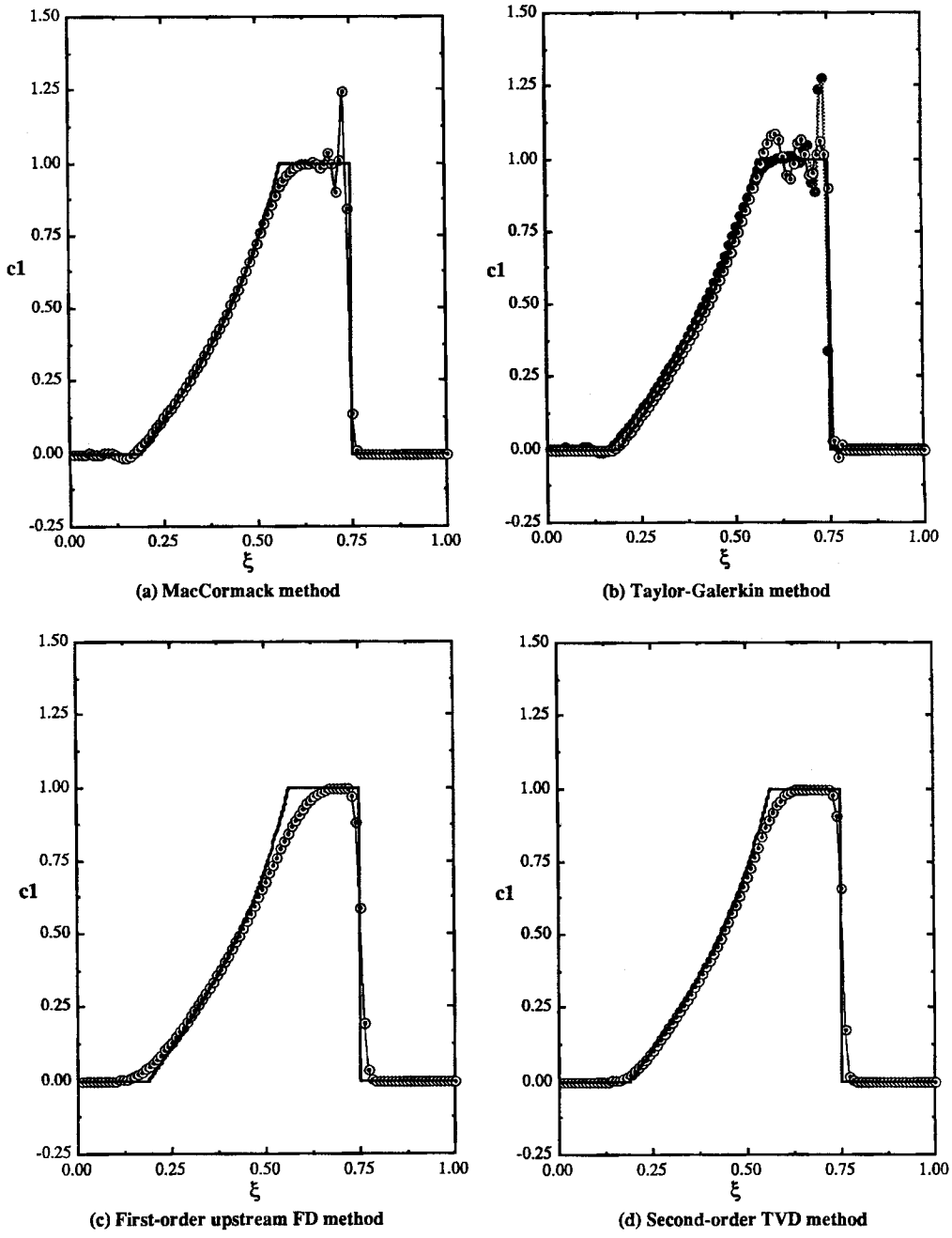

Figure 3. Typical numerical solutions (line with symbols) to the test problem of Section 1 compared to the exact solution (plain line). (b) Taylor–Galerkin method with lumped time derivatives (black circles) and without lumping (clear circles). For all figures: $c_{in}=1$, $\tau_{in}=0{\cdot}75$, $\tau_{obs}=2\tau_{in}$, $\alpha=2$, $K=2$, $\varepsilon=1{\cdot}5$. For figures (a)–(g): $\Delta\xi=1/100$, $\Delta\tau/\Delta\xi=1$. For figure (h): $\Delta\xi_{min}=0{\cdot}001$, $\Delta\xi_{max}=0{\cdot}01$, $\Delta\tau_{max}/\Delta\xi_{max}=1$, the initial mesh has 102 nodes at $\xi=0, 0{\cdot}001, 0{\cdot}01, 0{\cdot}02$, etc.

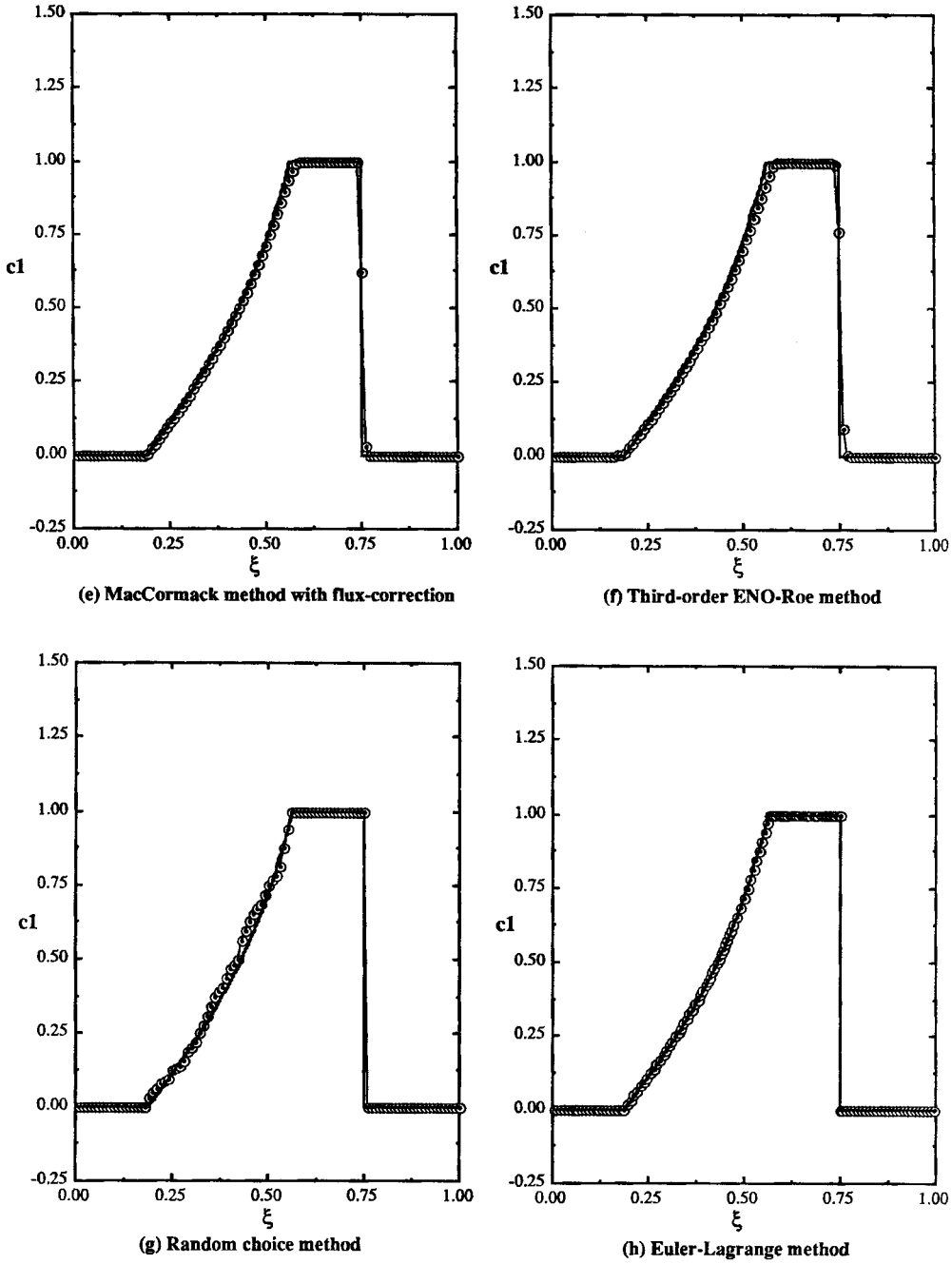

(e) MacCormack method with flux-correction

(f) Third-order ENO-Roe method

(g) Random choice method

(h) Euler-Lagrange method

Figure 3. (Continued)

representation of the shock discontinuity. In both cases, the front is as sharp as the minimum spatial grid spacing allows it to be. For the random choice method, the trailing wave exhibits wiggles which are inherent to the randomness of the scheme. With the Euler–Lagrange method the largest part of the error comes from the approximation of the rarefaction wave. This is due to the fact that, as nodes get too far apart, new points have to be added (linear interpolation was used) in order to keep a good resolution. At the same time, however, some error is introduced.

To analyse more precisely the accuracy of each numerical method, the error is defined as the 1-norm of the difference between numerical and exact solution

$$\text{Error} = \int_0^{\xi_d^-} |c_1 - c_{1,\text{ex}}| \, d\xi + \int_{\xi_d^+}^1 |c_1 - c_{1,\text{ex}}| \, d\xi, \tag{29}$$

where ξ_d designates the exact location of the discontinuity. Each of the above integrals was evaluated with the trapezoidal rule. For each method, five calculations were carried out on an Apollo DN 2500 workstation. The ratio $\Delta\tau/\Delta\xi$ was kept constant, while the number of grid points was varied from 51 to 101, 201, 401 and 801 (For the Euler–Lagrange method this was the initial number of nodes). The error evaluated for each case is plotted versus the computational time in Figure 4.

Ideally, we would like the methods to lie in the lower left quadrant. In practice, however, the Error vs. CPU time curves lie on a diagonal going from the upper left corner to the lower right corner of the graph. In the situation represented in Figure 4, we see that the logarithm of the error is roughly a linear function of the logarithm of the computational cost. Figure 4 also helps visualizing the computational cost associated with each method. Among the schemes using a fixed mesh, the first-order upstream finite difference and random choice methods are the fastest for the same number of grid points. On the other hand, the sophistication of the high-resolution methods results in high computational cost. For instance, when 201 grid points are used, the FCT, TVD and ENO methods are, respectively, about 4, 6 and 11 times slower than the random choice method. For the same situation, the FCT algorithm is about 1·5 times slower than the plain MacCormack method. However, the extra time spent by high-order methods usually results in a significant improvement of the accuracy of the computed solution. For example, Figure 4 shows that, among the fixed mesh methods, the most precise is the FCT scheme. With a mesh of 201 nodes, the flux-corrected MacCormack method gives an error of $4{\cdot}4 \times 10^{-3}$. In the same situation, the random choice, ENO, TVD, MacCormack, Taylor–Galerkin, Taylor–Galerkin with lumped time derivatives and upstream finite difference methods led to an error which is 1·3, 1·4, 2·0, 2·1, 2·2, 2·4 and 3·5 times bigger, respectively.

Comparison between moving mesh and fixed mesh methods is complicated by the fact that each set of methods uses different numerical parameters. For instance, the Euler–Lagrange method does not use a constant time-step or a fixed number of nodes. Instead, a maximum time-step is specified and the distance between two nodes is kept in an interval $[\Delta\xi_{\min}, \Delta\xi_{\max}]$. In addition, the moving mesh does not need to be uniform at the initial time. Nevertheless, to provide a comparison with the fixed grid methods, we decided to use the Euler–Lagrange method with an initially uniform mesh. At the starting time, the nodes are separated by $\Delta\xi_{\min}$ and $\Delta\xi_{\max}$ is set to $2\Delta\xi_{\min}$. The maximum time-step is chosen so that $\Delta\tau_{\max}/\Delta\xi_{\max}$ equals the value of $\Delta\tau/\Delta\xi$ for the fixed mesh techniques, that is $\Delta\tau_{\max}/\Delta\xi_{\max} = 0{\cdot}75$ in Figure 4. The Error vs. CPU time diagram shows that the explicit Euler–Lagrange method performs very well. For the test problem considered it is the second most accurate scheme behind the flux-corrected MacCormack method. With 201 nodes initially, the final error is $5{\cdot}6 \times 10^{-3}$. Finally, the Euler–Lagrange method is rapid although it is not the fastest.

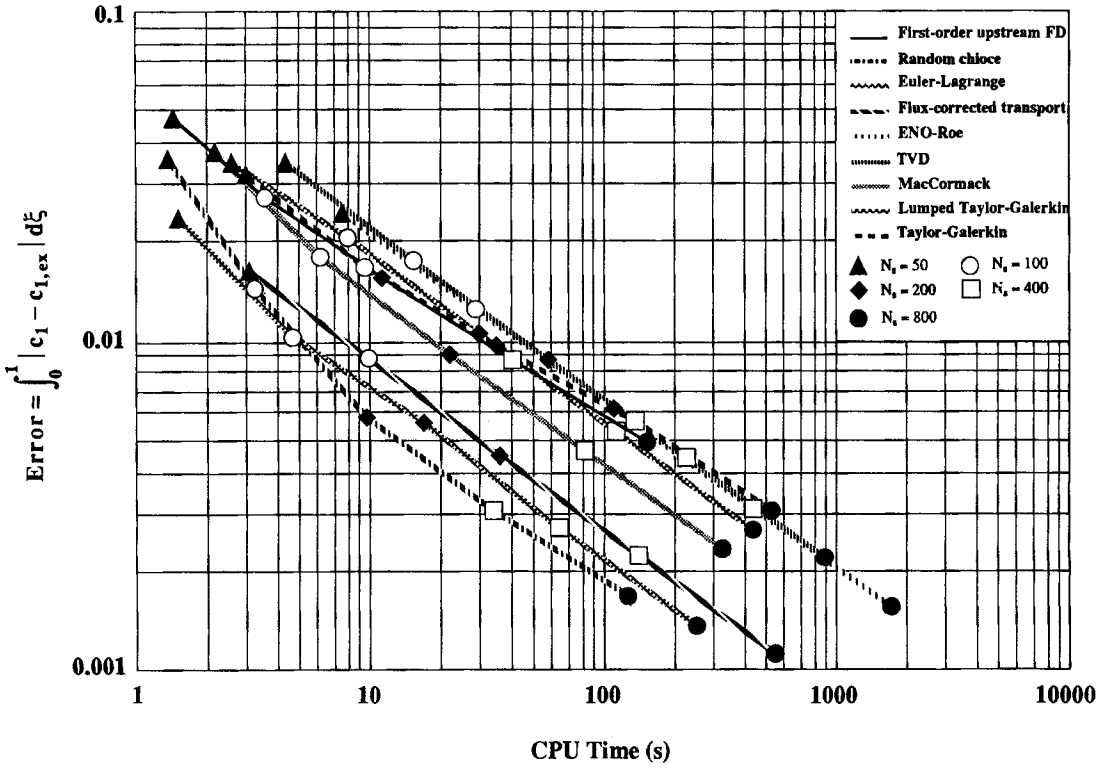

Figure 4. Error versus computational time for the test problem of Section 1. $c_{in}=1$, $\tau_{in}=0{\cdot}75$, $\tau_{obs}=2\tau_{in}$, $\alpha=2$, $K=2$, $\varepsilon=1{\cdot}5$. For the fixed grid methods: $\Delta\xi=1/N_s$, $\Delta\tau/\Delta\xi=0{\cdot}75$. For the Euler–Lagrange method, the initial grid is uniform with N_s grid points and $\Delta\xi_{min}=1/N_s$, $\Delta\xi_{max}=2\Delta\xi_{min}$, $\Delta\tau_{max}/\Delta\xi_{max}=0{\cdot}75$.

Figure 4 is certainly helpful in determining which method is the best for this application. For example, let us imagine that we need to solve the ideal chromatography problem but that we cannot accept an absolute error greater than 0·002. Then from Figure 4, we see that the random choice method will be the fastest method to provide an acceptable solution, but the number of nodes needed will be close to 800. The flux-corrected MacCormack method will be the third fastest but it will require less memory space since just over 400 nodes will be sufficient to reach the 0·002 accuracy level. The Euler–Lagrange method would also be suited for such an application. The other methods, however, would clearly be inefficient.

Of course, graphs such as Figure 4 can only give suggestions as to the best method. This is because the numerical parameters can take a great number of values, and each choice influences the performance of the numerical methods. For instance, to improve the computational time. one can increase the time-step while keeping the number of nodes constant. In general, this will lower the accuracy of the numerical approximation but, if $\Delta\tau$ becomes too big, the method will eventually oscillate and grow unstable.

Chromatographic column with axial diffusion

When diffusion is brought into the chromatographic model, the physical and numerical problems are completely changed. Figure 5 illustrates the effect of axial diffusion on the efficiency

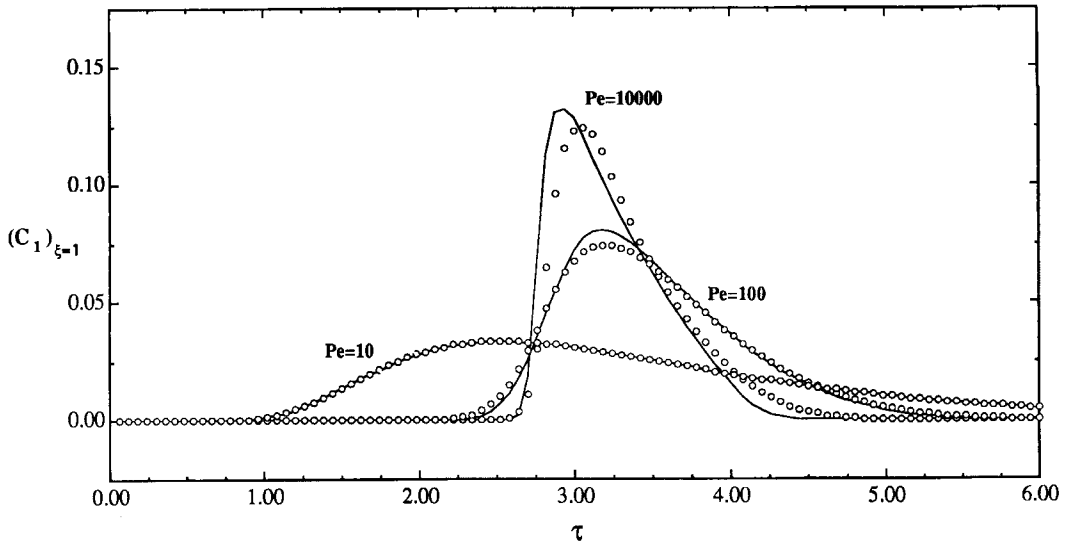

Figure 5. Effect of axial diffusion on the outflow concentration curves. Response to a pulse (equation (5)) with $c_{in}=1$, $\tau_{in}=0{\cdot}1$, $\alpha=2$, $K=2$, $\varepsilon=1{\cdot}5$. Solutions shown are for the ENO–Roe method (plain line) and TVD method (symbols). $\Delta\xi=1/50$, $\Delta\tau/\Delta\xi=1/20$.

of the chromatographic process. In this figure, the ENO–Roe and TVD methods have been used to model the response of the column to an injection of solute when the Péclet number varies from 10000 to 10. The results of the simulation reflect what one should expect from physical considerations. When the column is very efficient (high *Pe* number), the pulse remains narrow with smoothed but steep edges. As diffusion increases, however, the band of solute becomes broader and steep concentration gradients disappear.

Because of non-linearities, it is possible for steep gradients to develop in the presence of a significant amount of axial diffusion. This is shown in Figure 6 where, as the injection concentration is raised from 1 to 5, the band of solute becomes more and more asymmetrical. At the same time, the front edge of the non-linear wave becomes sharper, possibly leading to numerical difficulties.

Figures 5 and 6 also show how results obtained with different methods compare. In Figure 5 the same parameters have been used for both methods. In the absence of steep gradients, the two solutions agree very well. As the Péclet number is raised, however, the two curves become different. This reveals the lesser accuracy of the TVD scheme and its inability to keep the front sharp. As the grid is further refined, visual observation indicates that both methods converge to a unique solution, but the ENO scheme reaches convergence with fewer grid points.

With axial diffusion included in the model, there is no exact solution one could use to study thoroughly the computational efficiency of the numerical methods. Nevertheless, it appears that the conclusions drawn from Figure 4 remain valid but a few modifications need to be made when a sharp front develops in the presence of significant dispersion, as in Figure 6. In such a situation, methods that require an important number of mesh points to produce accurate results are penalized. This stems from the fact that, with diffusion, a practical stability condition is $\Delta\tau \leq \beta Pe\Delta\xi^2/2$, where β is a parameter that depends on the particular scheme used. Therefore, as $\Delta\xi$ is decreased, the computational time grows much faster than in the ideal case where

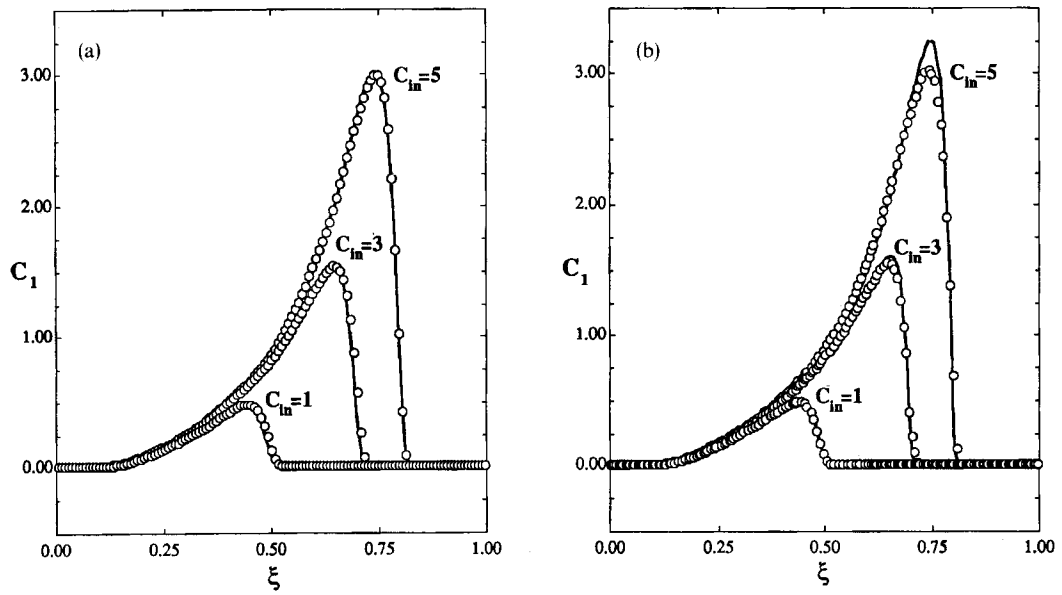

Figure 6. Effect of non-linearity. Response to a pulse (equation (5)) of increasing intensity: $c_{in}=1, 3$ and 5, $\tau_{in}=0{\cdot}25$, $\tau_{obs}=4\tau_{in}$, $\alpha=2$, $K=2$, $\varepsilon=1{\cdot}5$. Solutions shown are for (a) the MacCormack method with flux-correction (plain line, $Pe=200$, $\Delta\xi=1/80$ and $\Delta\tau/\Delta\xi=1/2$) and the random choice method (symbols, $Pe=200$, $\Delta\xi=1/125$ and $\Delta\tau/\Delta\xi=1/2$); and (b) the explicit Euler–Lagrange method (symbols, $Pe=200$, uniform initial mesh with 201 nodes, $\Delta\xi_{min}=1/200$, $\Delta\xi_{max}=2\Delta\xi_{min}$, $\Delta\tau_{max}/\Delta\xi_{max}=0{\cdot}4$) and the first-order upstream finite difference method (plain line, $Pe=400$, $\Delta\xi=1/200$ and $\Delta\tau/\Delta\xi=1/2$).

the time-step is limited by an expression analogous to the CFL condition (except for the Euler–Lagrange method). For the case of Figure 6 when $c_{in}=5$, the flux-corrected MacCormack method required only 8·6 CPU seconds and 81 grid points to produce a concentration curve that did not change (within plotting accuracy) when a finer mesh was used. To match that curve, it was necessary to use 126 nodes with the random choice method and the computational time was slightly higher at 10·4 s. The Euler–Lagrange scheme required even more nodes (165 nodes in the final curve) and the computational cost jumped to 32·0 s. It is worth noting that for these two methods, significant errors in the prediction of mass occur if the mesh has too few nodes. This is likely due to the presence of the non-linear function, $\sigma(c_1)$, in the diffusion term. For the particular problem of Figure 6, the ENO method was as efficient as the Euler–Lagrange method since the solution (not shown) it gave with $\Delta\xi=0{\cdot}01$ matched the FCT solution for $c_{in}=5$ and was obtained in a CPU time of 32·6 s. The performance of the other schemes were not as good. In particular, a more practical approach with the first-order upstream finite difference method is to compute the solution with Pe set to 400 instead of 200. Since with upwinding of the convection term, the dimensionless coefficient of diffusion is changed from $1/Pe$ to $1/Pe+\Delta\xi/2$, the amount of diffusion in the solution of Figure 6(b) really corresponds to a Péclet number of 200 ($1/200=1/400+0{\cdot}005/2$). With that adjustment, the first-order upstream method and the other methods agree quite well, except for the highest injection concentrations where the effect of non-linearity is more important and where the finite difference method predicts a slightly sharper front.

CONCLUSION

For one-dimensional non-linear, convective problems the random choice and explicit Euler–Lagrange methods are the most efficient schemes among those compared. The flux-corrected MacCormack method follows closely. However, for non-linear problems allowing the formation of steep fronts in the presence of significant diffusion, the FCT and random choice schemes appear to be the methods of choice. Obviously, there is not one single, best method among those we have investigated. Instead there are various good methods, each exhibiting different strengths and weaknesses. Naturally, such a study does not answer all the questions. For instance, how would the computational efficiencies of the methods compare for two-dimensional problems? This, however, is not a pressing concern for adsorption problems where complications come primarily from the increase in the number of (1) species, and/or (2) regions which are typically one-dimensional, or include a second dimension, but with *no* convection in that additional direction. We are confident that this study should be helpful in determining the most efficient method for similar applications.

ACKNOWLEDGEMENT

Support has been provided by N.I.H. through the Simulation Resource in Mass Transport and Exchange, directed by Dr. James B. Bassingthwaighte.

REFERENCES

1. B. A. Finlayson, *Numerical Methods for Problems with Moving Fronts*, Ravenna Park Publishing, Seattle, 1992.
2. K. Miller and R. N. Miller, 'Moving finite element methods. Part I', *SIAM J. Numer Anal.*, **18**, 1019–1032 (1981).
3. K. Miller and R. N. Miller, 'Moving finite element methods. Part II', *SIAM J. Numer. Anal.*, **18**, 1033–1057 (1981).
4. S. S. Hu and W. E. Schiesser, 'An adaptive grid method in the numerical method of lines', *Adv. Comp. Methods Partial Diff. Eqn.*, **IV**, 305–311 (1981).
5. M. D. Smooke and M. L. Koszykowski, 'Fully adaptive solutions of one-dimensional mixed initial-boundary value problems with applications to unstable problems in combustion', *SIAM J. Sci. Statis. Comput.*, **7**, 301–321 (1986).
6. C. A. J. Fletcher, *Computational Techniques for Fluid Dynamics I*, Springer, Berlin, 1988.
7. J. B. Bassingthwaighte, C. Y. Wang and I. S. Chan, 'Blood-tissue exchange via transport and transformation by capillary endothelial cells', *Circ. Res.*, **65**, 997–1020 (1989).
8. J. B. Bassingthwaighte, 'Through the microcirculatory maze with machete, molecule and minicomputer (1986 Alza lecture)', *Ann. Biomed. Eng.*, **15**, 503–519 (1987).
9. H.-K. Rhee, A. Rutherford and N. R. Amundson, *First Order Partial Differential Equations*: Vol. 1, Prentice-Hall, Englewood Cliffs, NJ, 1986.
10. J. B. Bassingthwaighte, 'A concurrent flow model for extraction during transcapillary passage', *Circ. Res.*, **35**, 483–503 (1974).
11. A. M. Lenhoff and E. N. Lightfoot, 'Convective dispersion and interphase mass transfer', *Chem. Eng. Sci.*, **41**, 2795–2810 (1986).
12. E. Suwondo, L. Pibouleau, S. Domenech and J. P. Riba, 'Simulation via orthogonal collocation on finite element of a chromatographic column with nonlinear isotherm', *Chem Eng. Comm.*, **102**, 161–188 (1991).
13. J. N. Wilson, 'A theory of chromatography', *J. Amer. chem Soc.*, **62**, 1583–1591 (1940).
14. D. DeVault, 'The theory of chromatography', *J. Amer. chem. Soc.*, **65**, 532–540 (1943).
15. P. Rouchon, M. Schonauer, P. Valentin and G. Guiochon, 'Numerical simulation of band propagation in nonlinear chromatography', *Separ. Sci. Technol.*, **22**, 1793–1833 (1987).
16. Z. Ma and G. Guiochon, 'Application of orthogonal collocation of finite elements in the simulation of non-linear chromatography', *Comput. Chem. Eng.*, **15**, 415–426 (1991).
17. G. A. Sod, *Numerical Methods in Fluid Dynamics*, Cambridge University Press, 1985.
18. R. J. LeVeque, *Numerical Methods for Conservation Laws*, Birkhäuser Verlag, 1992.
19. P. Lax and B. Wendroff, 'Systems of conservation laws', *Comm. Pure Appl. Math.*, **13**, 217–237 (1960).
20. R. W. MacCormack, 'The effect of viscosity in hypervelocity impact cratering', *AIAA Paper No. 69-354*, 1969.
21. D. A. Anderson, J. C. Tannehill and R. H. Pletcher, *Computational Fluid Mechanics and Heat Transfer*, MacGraw-Hill, New York, 1984.
22. J. Donea, 'A Taylor–Galerkin method for convective transport problems', *Int. j. numer. methods eng.*, **20**, 101–119 (1984).

23. J. Donea, S. Giuliani, H. Laval and L. Quartapelle, 'Time-accurate solution of advection–diffusion problems by finite elements', *Comp. Meth. Appl. Mech. Eng.*, **45**, 123–145 (1984).
24. B. A. Finlayson, *Nonlinear Analysis in Chemical Engineering*, McGraw-Hill, New York, 1980.
25. S. T. Zalesak, 'Fully multidimensional flux-corrected transport algorithms for fluids', *J. Comp. Phys.*, **31**, 335–362 (1979).
26. D. L. Book, J. P. Boris and K. H. Hain, 'Flux-corrected transport II: Generalization of the method', *J. Comp. Phys.*, **18**, 248–283 (1975).
27. D. L. Book, *Finite-Difference Techniques for Vectorized Fluid Dynamics Calculations*, Springer, Berlin, 1981.
28. A. Harten, 'High resolution schemes for hyperbolic conservation laws', *J. Comp. Phys.*, **49**, 357–393 (1983).
29. H. C. Yee, R. F. Warming and A. Harten, 'Implicit total variation diminishing (TVD) schemes for steady-state calculations', *J. Comp. Phys.*, **57**, 327–360 (1980).
30. P. K. Sweby, 'High resolution schemes using flux limiters for hyperbolic conservation laws', *SIAM J. Numer. Anal.*, **21**, 995–1111 (1984).
31. W. H. Chen, L. J. Durlofsky, B. Engquist and S. Osher, 'Minimization of grid orientation effects through use of higher order finite difference methods', *Soc. Pet. Eng. paper 22887*, 1991.
32. C. W. Shu and S. Osher, 'Efficient implementation of essentially non-oscillatory shock-capturing schemes', *J. Comp. Phys.*, **77**, 439–471 (1988).
33. C. W. Shu and S. Osher, 'Efficient implementation of essentially non-oscillatory shock-capturing schemes, II', *J. Comp. Phys.*, **83**, 32–78 (1989).
34. M. Holt, *Numerical Methods in Fluid Dynamics*, 2nd edition, Springer, Berlin, 1984.
35. J. Glimm, 'Solutions in the large for nonlinear hyperbolic systems of equations', *Comm. Pure Appl. Math.*, **18**, 697–715 (1955).
36. S. K. Godunov, 'Finite difference methods for numerical computation of discontinuous solutions of the equations of fluid dynamics', *Mat Sbornik*, **47**, 271 (1959).
37. A. J. Chorin, 'Random choice solution of hyperbolic systems', *J. Comp. Phys.*, **22**, 517–533 (1976).
38. A. J. Chorin, 'Random choice methods with applications to reacting gas flows', *J. Comp. Phys.*, **25**, 253–272 (1977).
39. G. A. Sod, 'A survey of several finite difference methods for systems of nonlinear hyperbolic conservation laws', *J. Comp. Phys.*, **27**, 1–31 (1978).
40. P. Concus and W. Proskurowski, 'Numerical solution of a nonlinear hyperbolic equation by the random choice method', *J. Comp. Phys.*, **30**, 153–166 (1979).
41. P. Colella, 'Glimm's method for gas dynamics', *SIAM J. Sci. Comput.*, **3**, 76–110 (1982).
42. G. Thomaidis, K. Zygourakis and M. F. Wheeler, 'An explicit finite difference scheme based on the modified method of characteristics for solving convection–diffusion problems in one space dimension', *Numer. Methods Partial Diff. Eqn.*, **4**, 119–138 (1988).